Available online at www.sciencedirect.com

SciVerse ScienceDirect

Journal of Nutritional Biochemistry 23 (2012) 469–477

Journal of Nutritional Biochemistry

Naringin, the major grapefruit flavonoid, specifically affects atherosclerosis development in diet-induced hypercholesterolemia in mice☆

Audrey Chanet[a,1], Dragan Milenkovic[a,1], Christiane Deval[a], Mylène Potier[b], Joël Constans[c], Andrzej Mazur[a], Catherine Bennetau-Pelissero[b], Christine Morand[a,*], Annie M. Bérard[c,*]

[a] INRA, UMR 1019, UNH, CRNH Auvergne, F-63000 Clermont-Ferrand ; Clermont Université, Université d'Auvergne, Unité de Nutrition Humaine, BP 10448, F-63000 Clermont-Ferrand
[b] Université de Bordeaux — ENITA Bordeaux 1, cours du Général de Gaulle 33 175 Gradignan cedex, France
[c] ERU «Facteurs de risque vasculaires», CHU-Université de Bordeaux, case 49, 146 rue Léo Saignat, 33076 Bordeaux, France

Received 23 November 2010; received in revised form 24 January 2011; accepted 1 February 2011

Abstract

Naringin (NAR) from grapefruit has exhibited potential protective effects against atherosclerosis development. However, specific mechanisms responsible for such effects are poorly understood. Thus, we aimed to investigate the antiatherogenic effects of NAR in different mouse models of hypercholesterolemia and decipher its molecular targets in the aorta using transcriptomic approach. Two mouse models of hypercholesterolemia, wild-type mice fed a high-fat/high-cholesterol diet and apolipoprotein E-deficient mice fed a semisynthetic diet, were studied. Mice were fed a respective control diets supplemented or not for 18 weeks with 0.02% of NAR, that is, nutritional supplementation. NAR supplementation reduced plaque progression only in wild-type mice fed the high-fat/high-cholesterol diet (−41%). Consistent with this protective effect, NAR reduced plasma non-high-density lipoprotein cholesterol concentrations as well as biomarkers of endothelial dysfunction. Microarray studies performed on aortas demonstrated differentially expressed genes encoding proteins involved in cell adhesion, actin cytoskeleton organization and cell division. Thus, the changes in gene expression induced by NAR could suggest a limited atherosclerosis progression by preventing immune cell adhesion and infiltration in the intima of vascular wall, as well as smooth muscle cell proliferation. Furthermore, this hypothesis was strengthened by *in vitro* experiments, which showed the ability of naringenin to reduce monocyte adhesion to endothelial cells and smooth muscle cell proliferation. In conclusion, this study revealed the antiatherogenic effect of NAR supplemented at a nutritionally achievable dose, specifically toward diet-induced atherosclerosis, and depicted its multitarget mode of action at the vascular level.

Keywords: Naringin; Flavonoid; Atherosclerosis; High-fat high-cholesterol diet; Hypercholesterolemic mouse models; Transcriptomic

1. Introduction

Atherosclerosis is a multifactorial disease of the large arteries and the leading cause of cardiovascular disease (CVD). Hypercholesterolemia, that is, increased plasma levels of low-density lipoprotein cholesterol (LDL-C), is a well-known risk factor involved in the induction of endothelial dysfunction, a key event in the pathogenesis of atherosclerosis. This endothelial dysfunction is initiated by an increase in the expression of chemotactic and adhesion molecules leading to recruitment of circulating cells to vascular endothelium and their migration into the arterial wall [1]. Moreover, smooth muscle cells (SMCs) migrate from media to intima and proliferate. Monocytes, which differentiate into activated macrophages, and SMCs, take up oxidized lipoproteins via scavenger receptors leading to the formation of foam cells. Gradual accumulation of foam cells in the intima results in fatty-streak formation corresponding to early-stage atherosclerotic lesions [1].

While there is a huge body of evidence on the positive association between high consumption of fruits and vegetables and a reduced risk of CVD [2], the specific role of the numerous plant bioactive molecules in these health effects is still under investigation. Among these phytochemicals, polyphenols, which constitute the most abundant dietary antioxidants, seem of particular interest regarding epidemiology. The Zutphen elderly study revealed an inverse association between mortality from CVD and the intake of flavonoids [3], a major subgroup of polyphenols. More recently, a prospective study yielded convincing results for an association between the dietary intake of flavanones as well as flavanone-rich foods and reduced risk of death due to coronary heart diseases [4]. Flavanones constitute a flavonoid

☆ This project has received funding from the French National Research Agency in the context of the National Program for Research on Food and Nutrition (ANR06-PNRA-013).

* Corresponding authors. Christine Morand is to be contacted at INRA centre de recherche de Clermont-Ferrand/Theix, Unité de Nutrition Humaine, Equipe Micronutriments, Métabolisme et Santé, 63 122 Saint-Genès-Champanelle, France. Tel.: +33 (0)4 73 62 40 84. Annie M. Bérard, CHU-Université Bordeaux, ERU «Facteurs de risque vasculaires», case 49, 146 rue Léo Saignat, 33076 Bordeaux, France. Tel.: +33 (0)5 56 79 56 79x14616.

E-mail addresses: christine.morand@clermont.inra.fr (C. Morand), annie.berard@u-bordeaux2.fr (A.M. Bérard).

[1] These authors contributed equally to this work.

0955-2863/$ - see front matter © 2012 Elsevier Inc. All rights reserved.
doi:10.1016/j.jnutbio.2011.02.001

subclass abundantly and specifically found in citrus [5], which could largely contribute to the total daily flavonoid intake [6].

Naringin (NAR), the glycosidic form of naringenin, constitutes the major flavanone found in grapefruit. In animal experiments, antiatherogenic effects of NAR or naringenin have been reported in hypercholesterolemic rabbits [7,8] and low-density lipoprotein (LDL) receptor knockout mice (LDLR−/−) fed a high-fat diet [9]. These studies also found that NAR or naringenin consumption was associated with lipid-lowering effects, reduced plasma markers of endothelial dysfunction and improved insulin sensitivity [7–9]. Such improvements have also been associated with changes in the activities of hepatic enzymes involved in cholesterol synthesis (3-hydroxy-3-methylglutaryl-coenzyme A [HMGCoA] reductase) and esterification acyl-coenzyme A-cholesterol acyltransferase (ACAT) in response to NAR [7,10], as well as changes in the expression of hepatic genes implicated in fatty acid oxidation and lipogenesis in response to naringenin [11,12]. Moreover, *in vitro* studies on HepG2 cells showed that naringenin, the aglycon compound released from NAR prior to its intestinal absorption, can inhibit apolipoprotein B (apoB)-containing lipoprotein secretion by reducing microsomal triglyceride transfer protein (MTTP) expression and activity and can increase the expression and activity of the LDLR [13,14]. Some of these effects might be mediated by the interaction of naringenin with the insulin signaling pathway [15,16]. Together with the impact on lipid metabolism, several *in vivo* and *in vitro* studies using various dietary flavonoids have shown their capacity to modulate vascular cell function through modulation of gene expression and intracellular signaling pathways [17–19].

Regarding NAR, even if animal studies suggested potential antiatherogenic effects, the physiological relevance of these studies is nevertheless arguable because most of them have been carried out using supranutritional doses [8,9]. Furthermore, the molecular mechanisms underlying the action of NAR have been mainly investigated through cell-culture experiments on targeted genes. However, the extrapolation of these mechanisms toward what is relevant *in vivo* is not directly possible. In this context, the aims of the present work were to evaluate the effects of NAR when supplemented in diets at a nutritional dose (0.02% wt/wt), on atherosclerosis development using two mouse models of hypercholesterolemia leading to atherosclerosis [wild-type (WT) mice fed a high-fat/high-cholesterol (HF-HC) diet, a model of diet-induced atherosclerosis [20,21] and apolipoprotein E knockout mice (apoE-/-) fed a standard diet], and to investigate the potential cellular and molecular mechanisms involved using microarray technology in the aorta. To support potential cellular targets of NAR revealed from microarray data, we also investigated the impact of its absorbable form, naringenin, on vascular cell function *in vitro*. In this way, we studied the effect of a nutritionally relevant concentration of naringenin on capacity of endothelial cells (ECs) to adhere monocytes and on SMCs proliferation.

2. Materials and methods

2.1. Mice and diets

As susceptibility to atherosclerosis is determined by both environmental and genetic factors, we used two dyslipidemic C57BL/6J mouse models of atherosclerosis: WT mice (Charles River Laboratories, L'Arbresle, France) on an HF-HC diet [22] and one spontaneous atherosclerotic mouse model, apoE−/− (Jackson Laboratories, Bar Harbor, MN, USA). Male mice were housed in a temperature-controlled (22±0.8°C) pathogen-free environment on a 12-h light/dark cycle, with free access to food and water. All animal experiments were performed according to the French Ministry of Agriculture Section of Health and Animal Protection (approval number 33-04476), the Institutional Ethics Committee of the french national institute for agricultural research (INRA) (decree number 87-848) and approved by Valorization Unit of the University of Bordeaux 2 under the agreement number R-45GRETA-F1-04. All procedures were carried out in compliance with the standards for use of laboratory animals. Mice were fed a standard breeding diet A03 (Safe, Epinay-sur-Orge, France) before the beginning of the experiment. After a 3-week adaptation period, 8-week-old mice from each mouse model were randomly divided into two groups and fed *ad libitum* for 18 weeks either an HF-HC diet (15% fat, 1.25% cholesterol, 0.5% cholic acid in cocoa butter diet with 75% Purina Mouse Chow #5015, TD.90221; Harlan Teklad, Tampa, FL, USA) or a standard semipurified diet [23], both of them supplemented or not with 0.02% of NAR (wt/wt) (Sigma, Saint-Quentin L'Abresles, France). At the end of the 18-week period, mice were killed under pentobarbital anesthesia.

2.2. Determination of plasma lipids, lipoproteins as well as markers of inflammation and endothelial dysfunction

Mice were fasted for 4 h, and blood was drawn from retro-orbital veins in the morning in tubes containing EDTA. Plasma samples were obtained by centrifugation at 2400*g* for 20 min at 4°C, separated and divided into aliquots, then stored frozen (−80°C) until analyzed.

Total cholesterol (TC) and triglycerides (TG) concentrations were measured using commercial enzymatic kits (bioMérieux, Marcy l'Etoile, France) as previously described [24]. High-density lipoprotein (HDL) were isolated from the supernatant obtained after selective precipitation of apoB-containing lipoproteins with phosphotungstic acid in the presence of magnesium ions and centrifugation. HDL cholesterol (HDL-C) was then quantified by enzymatic determination as above. To obtain a plasma lipoprotein profile, 500 μl of pooled fresh mice plasma was applied to a fast protein liquid chromatography (FPLC) system with two Superose columns connected in series (Pharmacia LKB, Orsay, France). Lipoproteins were eluted, collected and analyzed as previously described [24]. TC and TG were quantified in each fraction to establish an FPLC profile. Circulating markers of inflammation [interleukine-6 (IL-6)] and endothelial dysfunction [soluble vascular cell adhesion molecule-1 (sVCAM-1), soluble intercellular adhesion molecule-1 (sICAM-1) and soluble E-selectin (sE-selectin)] were determined by quantitative sandwich enzyme immunoassay technique (R&D Systems, Lille, France).

2.3. Determination of plasma antioxidant capacity and urinary isoprostanes

The ferric reducing ability of plasma (FRAP) was determined in fasted plasma collected on EDTA using the Benzie and Strain method with slight modifications [25]. Briefly, 20 μl of plasma diluted one fourth with bidistilled water was allowed to react with 200 μl of freshly made FRAP solution [300 mM acetate buffer (pH = 3.6), 8 mM tripyridyltriazine, 20 mM $FeCl_3$] in a 96-well microplate. The complex formed between reduced ferrous ions and tripyridyltriazine was quantified at 593 nm (Bio-Tek Instruments, Winooski, VT, USA), and the reaction was monitored for up to 4 min. In addition, 24-h urine 15-isoprostane F_{2t}, a marker of lipid peroxidation, was measured using a commercial ELISA kit (Oxford Biomedical Research, Oxford, MI, USA). Urinary 15-isoprostane F_{2t} concentrations were corrected for urinary creatinine levels. Briefly, urine was diluted 20 times, and the creatinine content was determined using an automated chemical analysis kit following the manufacturer's instructions (Kone Instruments Oyj, Espoo, Finland).

2.4. Analysis of aortic lesions

Atherosclerotic lesions were quantified as previously described [26,27]. Specimens were embedded in gelatin (Sigma) and sectioned with a cryostat at −20°C (Microm HM 560, Francheville, France). Serial sections of the aortic root and ascending aorta were performed at a thickness of 10 μm and stained with Oil red O and a hematoxylin counterstain (Sigma). Lesion size was then quantified using image analysis software starting from the aortic root and proceeding throughout the whole mount.

2.5. Microarray analysis

Aortas from mice were washed with physiologic saline solution maintained at 37°C by direct injection in the heart's left ventricle before collection. Each aorta from WT mice was collected in RNAlater (Sigma), and transcriptomic analysis was performed using pangenomic oligonucleotide Op Arrays (Operon, Cologne, Germany).

RNA extraction and fluorescent labeling. Aortas were placed in RNAlater to remove the surrounding adventitial fat tissue under an Olympus SZ40 Zoom Stereo Microscope (Olympus, Tokyo, Japan). Total RNA extraction was obtained from eight aortas: four aortas from mice that received the control diet and four aortas from mice that received the diet supplemented with NAR. RNA was extracted using the RNeasy Mini Kit (Qiagen, Hilden, Germany). RNA quality and quantity were checked by agarose gel electrophoresis and by the determination of the absorbencies at 260 and 280 nm on NanoDrop ND-1000 spectrophotometer (Thermo Scientific, Wilmington, DE, USA). RNA was amplified using Amino Allyl MessageAmp II aRNA Kit (Ambion, Austin, TX, USA) according to the manufacturer's instructions. Briefly, first-strand synthesis was carried out by reverse transcription using 1 μg of total RNA and T7 oligo(dT) primer. The aminoallyled antisense RNA amplification by T7 *in vitro* transcription was achieved at 37°C overnight. Amplified RNAs (aRNAs) were purified by application to an equilibrated filter cartridge and a second round of amplification was conducted (2 μg). Purified aRNAs (10 μg) from the second round of amplification were then fluorescently labeled with a Cy 5- or Cy 3-reactive dye (Cy Dye Post-Labeling Reactive Dye Pack; Amersham GE Healthcare, Buckinghamshire, UK) for 30 min at room temperature in the dark. The labeled aRNAs were purified by applying to equilibrated filters from an

RNeasy Mini kit (Qiagen). Quantities and labeling efficiencies of labeled aRNAs were determined by measuring the absorbencies at 260, 550 and 650 nm using a NanoDrop ND-1000 spectrophotometer.

Hybridization. Hybridization was carried out on the Operon mouse microarray (Operon). Array-Ready OligoSet Mouse Genome version 4.0 contains 35,852 longmer probes representing approximately 24,000 genes. Eight microarrays were used for a total of four independent comparisons. Hybridization was carried out in a Ventana hybridization system (Ventana Medical Systems, S.A, Illkirch, France) at 42°C for 8 h. Slides were subsequently washed twice in 2× and 0.1× saline sodium citrate at room temperature. The buffer remaining on the slide was removed by rapid centrifugation (4000*g*, 15 s). The fluorescence intensity was scanned using an Agilent Micro Array Scanner G2505B (Agilent Technologies, Inc., Santa Clara, CA, USA).

Image and data analysis. The signal and background intensity values for each spot in both channels were obtained using ImaGene 6.0 software (Biodiscovery, Inc., Proteigene, Saint-Marcel, France). Data were filtered using the ImaGene "empty spot" option, which automatically flags low-expressed and missing spots to remove them from the analyses. After base-2 logarithm transformation, data were corrected for systemic dye bias by Lowess normalization using GeneSight 4.1 software (BioDiscovery, Inc, Proteigene). Ratios were then filtered in accordance with their variability among the four comparisons, and genes with high variability were removed from the analysis. Statistical analyses were performed using the free R 2.1 software (http://www.r-project.org). The log ratio between NAR-supplemented and control samples was analyzed with Student's *t* tests to detect differentially expressed genes in the two nutritional conditions, and probability values were adjusted using a Bonferroni correction for multiple testing at 1% to eliminate false positives. Genes selected by these criteria are referred to as "differentially expressed genes." All data are MIAME (Minimum Information About a Microarray Experiment) compliant with raw data being deposited in the ArrayExpress database at the European Bioinformatics Institute under accession number E-MEXP-2932.

Gene ontology (GO) annotations of biological processes for differentially expressed genes were conducted using GOstat (http://gostat.wehi.edu.au) [28]. The program determines all annotated GO terms for all the genes and Fisher's Exact Test is performed to evaluate whether the observed difference is significant or not. The Benjamini and Hochberg correction is also performed to control the false discovery rate. To extract maximum biological information of differentially expressed genes, together with GO, genes were also classified according to their role(s) in cellular or metabolic pathways using both Kyoto Encyclopedia of Genes and Genome (KEGG) pathway tool (http://www.genome.jp/kegg/tool/color_pathway.html) and Ingenuity Pathway Analysis (IPA) (https://analysis.ingenuity.com).

2.6. Naringenin effects on HUVECs in vitro

Primary human umbilical vein ECs (HUVECs; Lonza, Walkersville, MD, USA) were used at passage 5 or 6 and were cultured in a phenol red-free endothelial growth medium supplemented with 2% fetal bovine serum, 0.4% fibroblast growth factor, 0.1% vascular endothelial growth factor, 0.1% heparin, 0.1% insulin-like growth factor, 0.1% ascorbic acid, 0.1% epidermal growth factor and 0.04% hydrocortisone (all from Lonza).

A monocytic cell line (U937) (ATCC, Manassas, VA, USA) was cultured in an RPMI medium (Pan Biotech, Aidenbach, Germany) supplemented with 2% fetal bovine serum (Sigma). Monocytes adhesion to HUVECs was investigated, as previously described [29]. Briefly, HUVECs were seeded in 24-well tissue culture plates and were allowed to proliferate until they reached 60%–70% confluence. The medium was then replaced to expose HUVECs for 24 h to an experimental medium containing vehicle (ethanol 0.5‰, control wells) or physiological concentrations of naringenin (1μM; Extrasynthèse, Genay, France). At the end of this period, the confluent monolayer was stimulated for 4 h with tumor necrosis factor α (TNF-α; 0.1 ng/ml; R&D Systems). Then 50 μl of a 5×10^6 U937 cell suspension was added to each well, and cells were further incubated for 1 h. The nonadherent U937 cells were rinsed off, and the wells were fixed with crystal violet in methanol (Sigma). The number of attached U937 cells was counted for each well in three random microscopic fields defined by an eyepiece. Triplicates for each condition were performed in three independent experiments.

2.7. Naringenin effects on mouse ASMCs in vitro

Aortic SMCs (ASMCs) were isolated from WT mice fed an HF-HC diet without supplementation in NAR. At sacrifice, a fragment of aorta was immediately placed at 37°C in a Dulbecco's modified Eagle's medium (DMEM; Sigma) containing 20% fetal calf serum (FCS) (Sigma) for ASMCs isolation as previously described [30]. After three passages, the cells were characterized by positive staining with antismooth muscle α-actin, and cells were subcultured in DMEM supplemented with 20% FCS and used between passages 4 and 12. To examine naringenin's effect on cell proliferation, ASMCs were plated and maintained for 24 h in a DMEM containing 20% FCS. The medium was replaced for 24 h with a phenol red-free medium supplemented with 2.5% charcoal-stripped FCS (experimental medium). Then the medium was replaced by an experimental medium containing vehicle (ethanol 0.1‰, control wells) or naringenin (1 μM). Proliferation was assessed by determining cell number at days 1, 3 and 5 with a Coulter cell counter. Proliferation was determined on two different primary cell lines obtained from two WT mouse aortas. For each line, assays were performed in duplicate in three independent experiments.

2.8. Statistical analyses

A one-way analysis of variance coupled with a multiple comparison test was used to compare effects of diets between them. $P<.05$ was taken to imply statistical significance.

3. Results

3.1. Effects of NAR on atherosclerosis development

The extent of atherosclerotic lesions differed greatly between the two mouse models, with apoE−/− animals having a lesion area ten times higher compared with WT mice fed the HF-HC diet (Fig. 1). A significant reduction in atherosclerotic lesions after NAR supplementation was only observed in WT mice fed the atherogenic diet (−41%).

3.2. Effects of NAR on plasma lipid profile

Compared with WT mice on a standard mouse diet ($n=15$), those on an HF-HC diet ($n=15$) showed a marked increase in plasma non HDL-C concentrations (+274%; $P<.0001$) associated with a significant decrease in plasma HDL-C (−45%; $P<.001$), as expected [31]. The increase in non-HDL-C reflected that of very-low-density lipoprotein (VLDL) and IDL(intermediate-density lipoprotein)/LDL when analyzed by FPLC (data not shown). This diet also induced a decrease in plasma TG (−40%; $P<.001$), as observed elsewhere [20]. Compared with WT mice on the HF-HC diet, apoE−/− mice displayed a 1.9-fold increase in plasma concentrations of TC and TG (Table 1).

In WT mice on the HF-HC diet, NAR decreased plasma TC by 13% and improved TC/HDL-C ratio due to a 20% reduction of non-HDL-C without affecting HDL-C concentrations (Table 1). Furthermore, analysis of the plasma lipoproteins by FPLC demonstrated that NAR-treated mice presented less VLDL (Fig. 2). Overall, the supplementation with NAR at

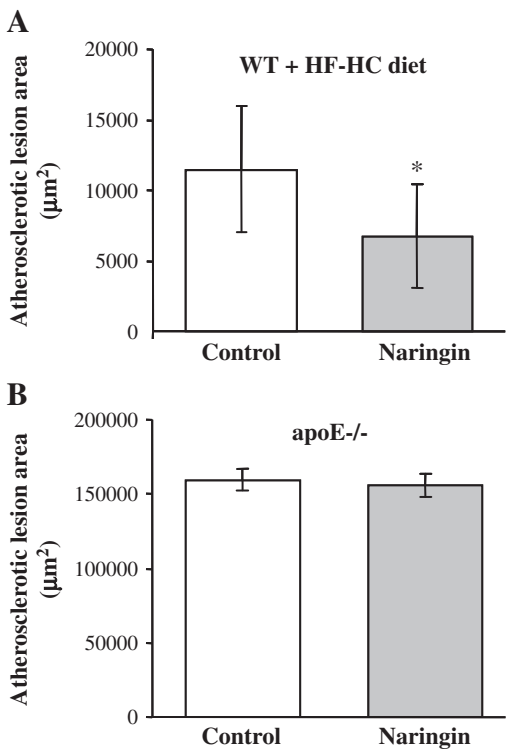

Fig. 1. Size of atherosclerotic lesions after an 18-week supplementation period with 0.02% NAR in WT mice fed an HF-HC diet ($n=12$; A) or in apoE-/- on a standard semisynthetic diet ($n=12$; B). Values are means±S.E.M., *$P<.05$ versus control.

Table 1
Plasma lipid concentrations after an 18-week supplementation period with 0.02% NAR in WT mice fed an HF-HC diet or in apoE-/- on a standard semisynthetic diet

	WT on HF-HC diet		ApoE−/− on semisynthetic diet	
	Control	NAR	Control	NAR
TG (mg/dl)	46±5	41±4	88±7	85±3
TC (mg/dl)	151±21	132±13 *	279±14	281±11
HDL-C (mg/dl)	36±5	39±7	22±1	26±3
Non-HDL-C (mg/dl)	116±20	93±9 *	257±13	255±11
TC/HDL-C	4.3±0.8	3.5±0.5 *	13.0±1.1	12.5±1.5

Values are means±S.E.M. (n=15 per group for WT mice on the HF-HC diet, n=12 per group for apoE−/− mice).
* P<.05 versus control.

Table 2
Markers of cardiovascular risk after an 18-week supplementation period with 0.02% NAR in WT mice fed an HF-HC diet

	Control	NAR
Endothelial dysfunction		
sVCAM-1 (ng/ml)	1230±84	1128±107
sICAM-1 (ng/ml)	1263±170	989±133 *
sE-selectin (ng/ml)	54±11	33±6 **
Inflammation: IL-6 (pg/ml)	18±8	12±5
Oxidative stress/ antioxidant status		
FRAP (μM)	487±38	527±35
Urinary isoprostanes (pg/μg of creatinin)	15.9±1.5	14.8±1.1

Values are means±S.E.M. (n=15 per group).
* P<.001.
** P<.0001 versus control.

a nutritional dose resulted in a less atherogenic plasma lipid profile in WT mice on the HF-HC diet. In contrast, in apoE−/− mice, NAR did not modify plasma lipids (Table 1).

3.3. Effects of NAR on plasma markers of endothelial dysfunction and inflammation as well as oxidative stress parameters in WT mice fed the HF-HC diet

Quantification of soluble forms of adhesion molecules in plasma showed that NAR decreased sE-selectin concentrations by 39% and sICAM-1 concentrations by 22% in WT mice fed the HF-HC diet (Table 2). By contrast, no changes in plasma levels of IL-6 or plasmatic antioxidant capacity (FRAP) or urinary 15-isoprostane F_2 concentrations were observed in response to NAR supplementation (Table 2).

3.4. Impact of NAR on gene expression in the aorta of WT mice fed the HF-HC diet

To identify potential molecular mechanisms of NAR *in vivo*, transcriptomic analysis of the aorta was performed. Using this approach, expression of 1417 genes was identified as differentially expressed following NAR supplementation (Supplemental Table 1). Among these 1417 genes, 714 genes were identified as up-regulated and 703 genes were down-regulated after NAR consumption, with magnitude of FC ranging from 1.24 to 3.66 and −1.22 to −3.66, respectively. For selected genes involved in cell adhesion and cytoskeleton organization, microarray results were confirmed by real-time reverse transcriptase polymerase chain reaction amplification (data not shown).

To decipher biological processes affected by NAR supplementation, the list of differentially expressed genes was subjected to gene-annotation enrichment analysis using GOstat bioinformatics resources. The list of GO groups of biological processes, which are highly represented, is presented in Table 3. This analysis revealed that differentially expressed genes are implicated in different processes, such as metabolic processes, signaling cascade or cell cycle process. Among the processes identified, several of them had genes implicated in cell adhesion, regulation of actin polymerization/depolymerization, regulation of actin filament length, regulation of actin cytoskeleton organization and biogenesis, as well as genes implicated in cell cycle, mitosis and cell division. To further refine biological function in which differentially expressed genes are implicated, we placed the genes according to their role(s) in cellular or metabolic pathways. We used the KEGG and Ingenuity System to carry out analyses for both up- and

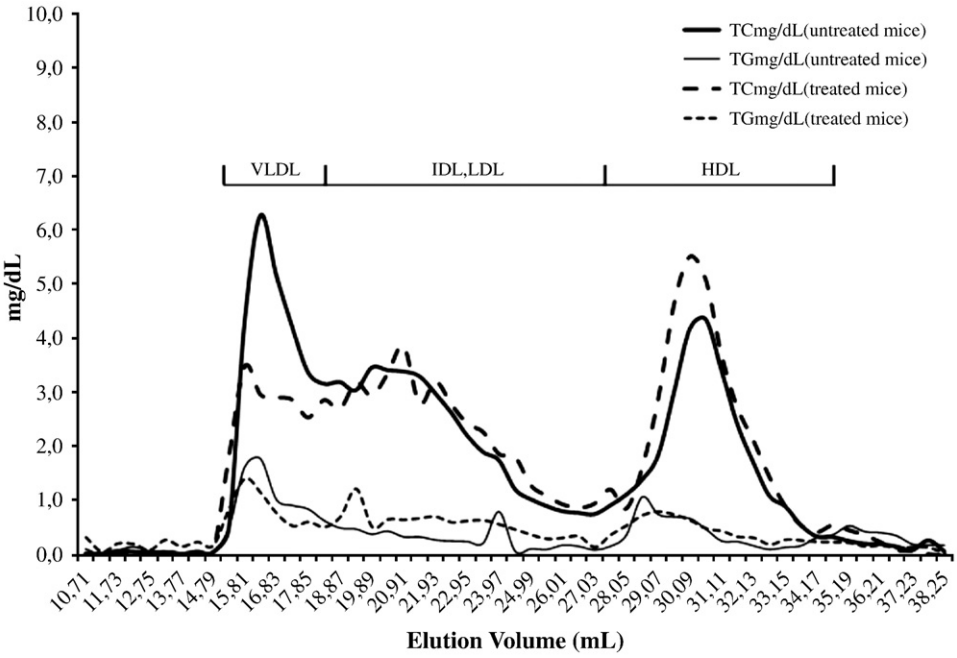

Fig. 2. TC and TG distribution in the plasma lipoproteins from WT mice fed an HF-HC diet supplemented with 0.02% of NAR (treated mice, n=15) or not (untreated mice, n=15). The elution positions of VLDL, IDL/LDL and HDL lipoproteins are indicated.

Table 3
Functional enrichment analysis based on GO biological process terms of differentially expressed genes in aorta of WT mice fed an HF-HC diet supplemented with 0.02% of NAR

GO accession no.	GO name	*P*
GO:0044237	Cellular metabolic process	.0001
GO:0044238	Primary metabolic process	.0001
GO:0065007	Biological regulation	.0052
GO:0050794	Regulation of cellular process	.0069
GO:0000279	M phase	.0069
GO:0007264	Small GTPase-mediated signal transduction	.0093
GO:0043170	Macromolecule metabolic process	.0093
GO:0007608	Sensory perception of smell	.0093
GO:0007606	Sensory perception of chemical stimulus	.0093
GO:0006259	DNA metabolic process	.0109
GO:0022402	Cell cycle process	.0109
GO:0043283	Biopolymer metabolic process	.0131
GO:0051128	Regulation of cellular component organization and biogenesis	.0131
GO:0007600	Sensory perception	.0149
GO:0050789	Regulation of biological process	.0149
GO:0006139	Nucleobase. nucleoside. nucleotide and nucleic acid metabolic process	.0149
GO:0007049	Cell cycle	.0149
GO:0051261	Protein depolymerization	.0174
GO:0007067	Mitosis	.0174
GO:0009165	Nucleotide biosynthetic process	.0174
GO:0007186	G-protein-coupled receptor protein signaling pathway	.0174
GO:0051246	Regulation of protein metabolic process	.0174
GO:0000087	M phase of mitotic cell cycle	.0175
GO:0045785	Positive regulation of cell adhesion	.0175
GO:0022403	Cell cycle phase	.0175
GO:0007166	Cell surface receptor linked signal transduction	.0197
GO:0051129	Negative regulation of cellular component organization and biogenesis	.0197
GO:0051301	Cell division	.0197
GO:0000278	Mitotic cell cycle	.0244
GO:0016043	Cellular component organization and biogenesis	.0251
GO:0045598	Regulation of fat cell differentiation	.0251
GO:0006753	Nucleoside phosphate metabolic process	.0251
GO:0006754	ATP biosynthetic process	.0251
GO:0045595	Regulation of cell differentiation	.0297
GO:0006818	Hydrogen transport	.0412
GO:0050877	Neurological system process	.0416
GO:0015986	ATP synthesis coupled proton transport	.0416
GO:0015985	Energy-coupled proton transport. Down-electrochemical gradient	.0416
GO:0008064	Regulation of actin polymerization and/or depolymerization	.0416
GO:0022607	Cellular component assembly	.0416
GO:0008154	Actin polymerization and/or depolymerization	.0416
GO:0046034	ATP metabolic process	.0416
GO:0030832	Regulation of actin filament length	.0462
GO:0032535	Regulation of cellular component size	.0462
GO:0032956	Regulation of actin cytoskeleton organization and biogenesis	.0462
GO:0003008	System process	.0462
GO:0019222	Regulation of metabolic process	.0490
GO:0007242	Intracellular signaling cascade	.0490

down-regulated genes. Pathways identified from KEGG database are presented in Fig. 3. Pathways implicated in cell adhesion/communication, cellular signaling pathways and cellular metabolic pathways were identified. Similar pathways were also obtained using IPA (data not shown).

3.5. Modulation of monocyte adhesion to ECs and ASMCs proliferation by naringenin in vitro

The ability of naringenin, the absorbable form of NAR, to modulate ECs (HUVECs) function was assessed through *in vitro* adhesion assay experiments. Results showed that a 24-h pretreatment of HUVECs with 1 μM naringenin significantly reduced the adhesion of monocytes to TNF-α-stimulated HUVECs (−16%; Fig. 4). Moreover, a 72-h treatment of isolated ASMCs with 1 μM naringenin significantly decreased cell number when compared with the control medium (−25%; Fig. 5).

4. Discussion

The objectives of this study were to evaluate the effects of a nutritional supplementation in NAR on atherosclerosis development in two mouse models of hypercholesterolemia and to identify its molecular targets by using microarray technology. It should be highlighted that the dose of NAR daily consumed by mice corresponds to a human equivalent dose of 100 mg NAR. According to the Food Standard Agency, this amount of NAR may be provided by the consumption of 1.5 servings of grapefruit juice or by half a fruit. This supplementation level led to plasma naringenin concentrations in mice (Supplemental Table 2) that are close to those observed in humans consuming citrus juice [32,33].

Our study showed that different mouse models of atherosclerosis differ noticeably in their response to nutritional NAR supplementation particularly with regard to hyperlipidemia and atherosclerotic lesion extent. In WT mice fed the HF-HC diet, NAR led to a less atherogenic lipoprotein profile and to an atheroprotective effect, whereas NAR did not demonstrate any effect in apoE−/− mice. Such findings could reveal that NAR interferes with the hepatic removal of VLDL and VLDL remnants from plasma by mechanisms that involved apolipoprotein E (apoE) receptors as LDLR. In agreement with this assumption, previous works have shown that naringenin was able to increase the expression and activity of the LDLR in HepG2 cells [13,15,16]. By contrast, Mulvihill et al. [9] demonstrated an atheroprotective effect of naringenin in LDLR−/− mice. However, this last study had an experimental design markedly different from ours: first, the diet was supplemented with naringenin, which is the aglycon form of NAR, and second, naringenin was used at a pharmacological dose (300 times higher than ours). Also, previous studies indicated that LDLR is not rate limiting for the clearance of VLDL and their remnants [34] and that backup clearance of these lipoparticules could be mediated by LRP (LDL-related protein), which binds apoE-enriched remnant lipoproteins [35]. These observations, together with results obtained in our study, suggest that NAR might modulate the LRP pathway. Finally, as reported by others, reduced plasma lipemia after NAR supplementation might also originate from a decreased apoB-containing lipoprotein secretion [11,13,14]. As a matter of fact, it has been demonstrated that the inhibition of microsomal TG transfer protein activity by naringenin represents the primary mechanism responsible for the dramatic reduction in apoB lipidation and secretion [13,14]. The ability of NAR to modulate apoB secretion could also be related to its insulin-like action [11]. This latter hypothesis could be corroborated by our data showing that NAR corrected the insulin resistance induced by the high-fat component of the atherogenic diet (data not shown).

During the course of atherosclerosis, alteration of endothelial function is characterized by a rise in ECs adhesion molecule expression (E-selectin, VCAM, ICAM), leading to increased adhesion of immune cells to the endothelium, which facilitates their migration into the subendothelial space [1]. Previously, an atherogenic diet, similar to the one used in our study, has been shown to induce an increase in plasma levels of soluble forms of cell adhesion molecules in WT mice indicating an endothelial dysfunction [21]. In the present study, in mice on the HF-HC diet, NAR lowered plasma concentrations of soluble forms of cell adhesion molecules. This result is in agreement with another study in which NAR has been shown to reduce adhesion molecule expression despite the absence of changes in lipemia in HC-fed rabbits [7]. These observations suggest that NAR could attenuate endothelial dysfunction induced by an atherogenic diet. Furthermore, the transcriptomic analysis performed in the aorta revealed that NAR modulated the expression of genes involved in cell adhesion

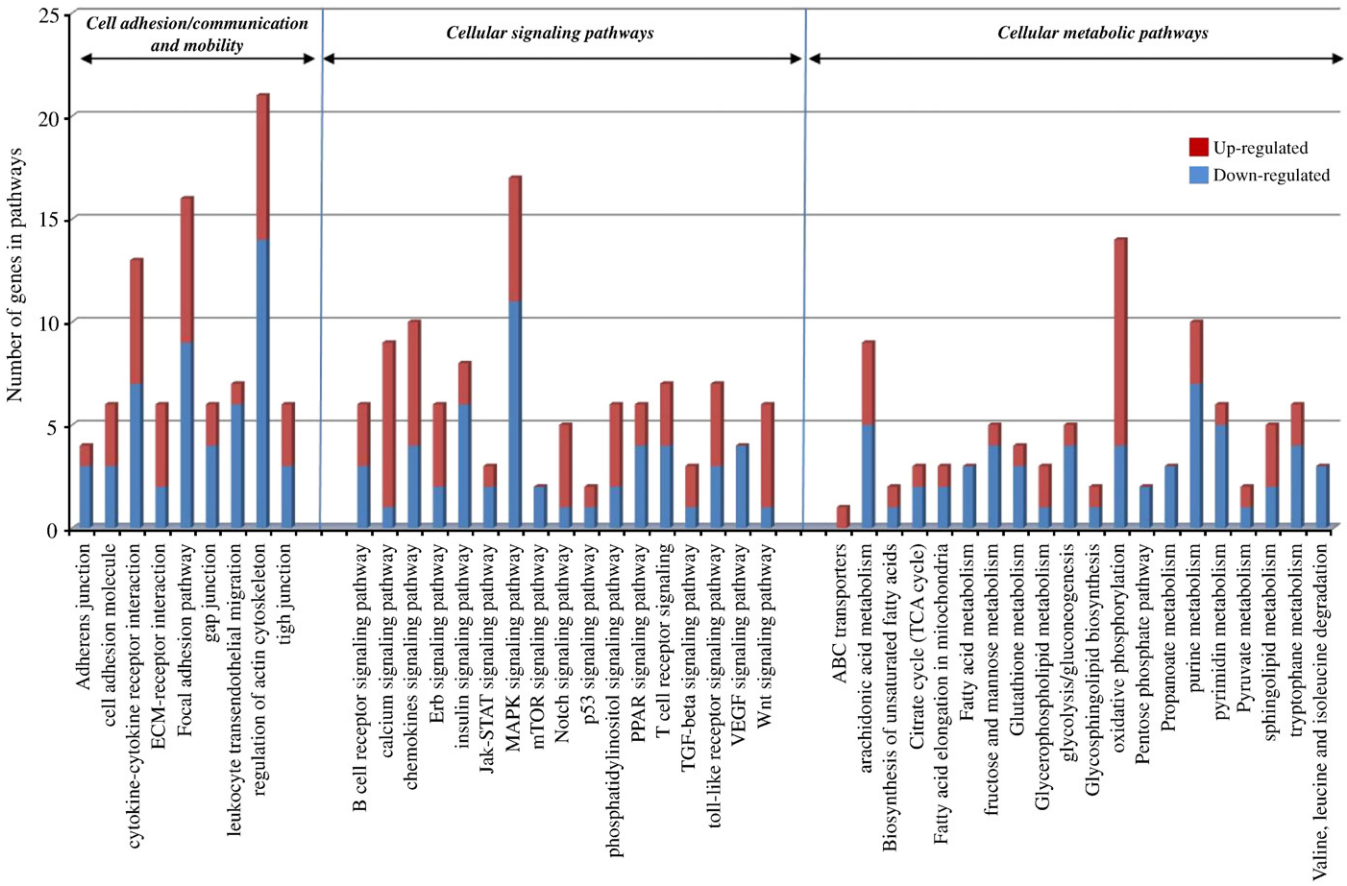

Fig. 3. Pathways affected by an 18-week supplementation period with 0.02% NAR in the aorta of WT mice fed an HF-HC diet. Differentially expressed genes were analyzed across pathways from KEGG database.

processes. GO analysis of microarray data pointed out 32 genes involved in this process. Among these genes, we observed a significant down-regulation of leukocyte adhesion molecule 1 (0.8) or Von Willebrand factor (0.76) known to be involved in initiation of adhesion of circulating white blood cells [36,37]. Together with genes coding for adhesion molecules, we also identified modulation of expression of genes coding for chemokines, small cytokine proteins involved in recruitment of leukocytes into vasculature [38]. Among these genes, a significant down-regulation was observed for chemokine ligand 8 (0.72), S100 calcium binding protein A9 (0.74) or chemokine-like factor 3 (0.8). Taken together, regarding the decrease of soluble cell adhesion molecules as well as expression of genes coding for cell adhesion molecules and chemokines, we can hypothesize that NAR supplementation may directly affect the activity of ECs, leading to a reduction of leukocyte adhesion to endothelium. This hypothesis was supported by our *in vitro*

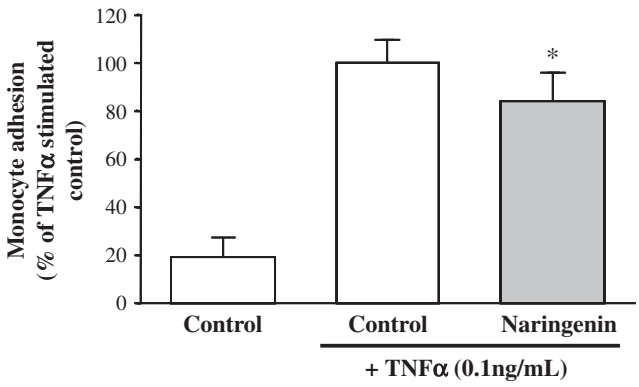

Fig. 4. Effect of naringenin on TNF-α-induced adhesion of monocytes (U937) to HUVECs. HUVECs were pretreated with vehicle (ethanol 0.5‰, control) or naringenin (1 μM) for 24 h and then stimulated or not with TNF-α (0.1 ng/ml) for 4 h before U937 addition. Values are means±S.D. from three independent experiments performed in triplicates, *P<.05 versus TNF-α-stimulated control.

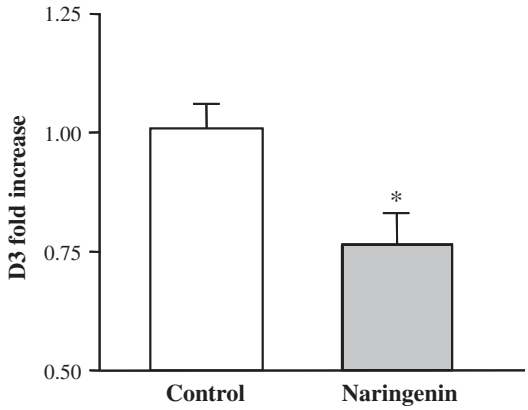

Fig. 5. Effect of naringenin on ASMCs number. ASMCs isolated from control WT mice fed an HF-HC diet were exposed for 72 h to vehicle (ethanol 0.1‰, control) or naringenin (1 μM). Values are means±S.D. from three independent experiments performed in duplicate, on two different primary cell lines, *P<.05 versus control.

experiment showing that the exposure of HUVECs to naringenin significantly reduced the adhesion of monocytes to ECs. The capacity of NAR to decrease monocyte adhesion may result in lowering monocyte accumulation in intima of aorta and, in consequence, leading to a lesser extent of lesion development, as we observed in aortic roots of mice supplemented with NAR.

Leukocyte adhesion to ECs induces cytoskeletal changes of these cells by forming "docking structures," or actin-rich membrane extensions that surround the adherent cells, this latter being regulated by ezrin/radixin/moesin proteins [39]. These cytoskeleton modifications could facilitate transendothelial migration either through or in-between ECs [40]. In addition, to facilitate migration, increased endothelial permeability will be driven by the rearrangement of the actin cytoskeleton and also by the activation of endothelial acto-myosin contractile machinery induced by myosin light chain (MLC) phosphorylation [41]. MLCs phosphorylation leads to stress fiber formation and subsequently to cell contraction that causes adjacent cells to retract from each other, increasing intercellular gaps and facilitating the entry of inflammatory cells [42]. Our microarray analysis has revealed that NAR supplementation modulated expression of numerous genes implicated in these steps of transendothelial migration (Table 3). Notably, NAR supplementation decreased the expression of genes coding for members of the arp2/3 complex (0.80) and radixin (0.79), both involved in actin filament organization. As described previously [43], a decreased expression of ezrin/radixin/moesin genes was associated with reduced endothelial permeability, a change that could reduce leukocyte infiltration. We also observed that nutritional dose of NAR decreased the expression of one of the genes encoding MLCs, myosin regulatory light chain 2-B (MYLC2B) (0.79). Blood cell adhesion to ECs has also been shown to activate the small GTP-binding protein Rho which can activate Rho-associated kinase, which in turn phosphorylates MLCs and induce stress fiber formation [44]. In our study, Rho guanine nucleotide exchange factor (*Arhgef12*) was observed to be down-regulated (0.69). Similarly, *cdc42*, a key gene belonging to Rho GTPase family, was also down-regulated by NAR supplementation. It has been previously reported that a decrease in *cdc42* in ECs may strengthen the endothelial barrier function [45] and reduce leukocyte migration [46]. Modulation of expression of genes coding for small GTPase by NAR could be associated with lower MLCs activation, stress fiber formation and subsequent cell contraction. These genes implicated in actin cytoskeleton, small GTP-binding protein and MLCs form network in cell cytoskeleton pathway as presented in the Fig. 6. This pathway was identified as the most significantly overrepresented by IPA analysis, making it an interesting molecular target of NAR. Taken together, these results suggest that NAR supplementation, by altering gene expression, may improve vascular integrity by attenuating blood cell adhesion and strengthening endothelial barrier. Such processes could be associated with limited atherosclerosis progression by preventing immune cell infiltration in the intima of vascular wall.

Recruitment of circulating inflammatory cells into the vascular wall triggers vascular SMCs proliferation and their migration into the intima where they differentiate and secrete extracellular matrix proteins [1]. Interestingly, among the different identified GO processes, several processes are also implicated in control of cell division, such as genes involved in M phase, cell cycle process, cell cycle, cell division and

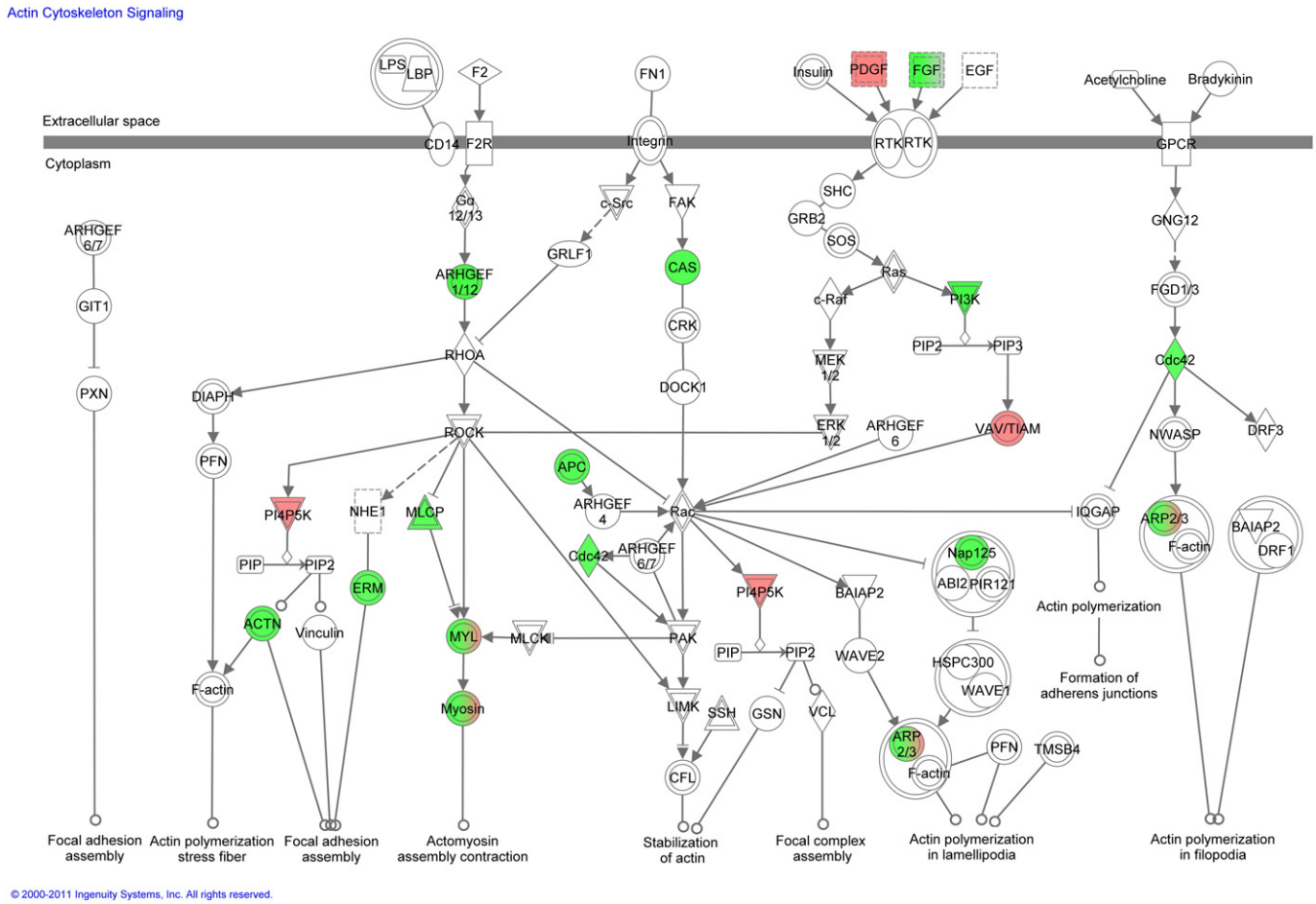

Fig. 6. Actin cytoskeleton signaling pathway, the top canonical pathway, determined by Ingenuity Pathway Analysis from differentially expressed genes in aorta of WT mice fed an HF-HC diet supplemented with 0.02% NAR. Color coding: red, up-regulated genes; green, down-regulated genes.

mitotic cell cycle (Table 3). Among the genes identified in cell cycle, we observed a down-regulation of expression of gene coding for signal transducer and activator of transcription 5B (STAT5B). This transcription factor has been shown to play a role in vascular SMCs growth and proliferation, and suppression of its expression has been shown to block growth and mobility of these cells [47]. In addition to STAT5B, NAR supplementation at nutritional dose also repressed expression of three genes coding for cyclins: cyclin B2 (0.73), cyclin-dependent kinase 9 (0.71) and cyclin A2 (0.67). Cyclins are a family of proteins that control the progression of cells through the cell cycle. A decrease in high-glucose-induced expression of cyclins in human ASMCs has been associated with a decreased cell proliferation [48]. Together with the down-regulation of expression of genes coding for proteins controlling the progression of cells through the cell cycle, we also observed an increase in the expression of *wee1* (1.24), gene coding for a protein known to inhibit the entry into mitosis. It has been previously observed that suppression of WEE1 expression induced rat ASMCs proliferation [49]. Furthermore, expression of gene coding for fibroblast growth factor receptor 2 (FGFR2) was also identified as down-regulated by NAR in the aorta. *fgfr2* is expressed in the vascular SMCs of the media and thickened intima of atherosclerotic arteries and is potentially involved in the proliferation of these cells [50]. Taken together, the observed expression profile for these genes suggests a decrease in proliferation of vascular SMCs in aorta of mice that regularly consumed NAR through the diet. This hypothesis could be corroborated by the observed *in vitro* ability of naringenin to reduce proliferation of SMCs isolated from WT mice fed the HF-HC diet. Overall, a reduction of SMCs proliferation by NAR would reduce vascular wall thickening and atherosclerosis development as observed in WT mice fed the HF-HC diet.

In conclusion, the present study demonstrates that NAR supplementation within a nutritional range specifically reduces diet-induced atherosclerosis in WT mice fed an HF-HC diet. This protective effect could be attributed to improved dyslipidemia and biomarkers of endothelial dysfunction, but also to changes in gene expression that may lead to preservation of the vascular wall, as shown by the aorta transcriptomic analysis. Our results highlighted molecular mechanisms brought into play by NAR in ECs and in SMCs, which could underlie its antiatherogenic effect. These latter mechanisms appear closely related to processes involved in leukocyte adhesion and transendothelial migration together with SMCs proliferation. In a future work, it would be of interest to evaluate if NAR exposure may lead to persistent effects after stopping the supplementation, as well as to determine if NAR supplementation might allow regression of established atherosclerotic lesions.

Supplementary materials related to this article can be found online at doi:10.1016/j.jnutbio.2011.02.001.

Acknowledgments

We thank the following people for their technical assistance: Valerie Lamothe from Ecole Nationale d'Ingénieurs des Travaux Agricoles de Bordeaux (ENITBAB), Aurélie Amadio and Antonio Palos-Pinto from the University of Bordeaux as well as Catherine Besson, Dominique Bayle, Séverine Thien and Philippe Denis from INRA. We also thank the Union Nationale Interprofessionnelle des Jus de Fruits (UNIJUS), which followed and communicated about this research program.

References

[1] Lusis AJ. Atherosclerosis. Nature 2000;407:233–41.
[2] Dauchet L, Ferrieres J, Arveiler D, Yarnell JW, Gey F, Ducimetiere P, et al. Frequency of fruit and vegetable consumption and coronary heart disease in France and Northern Ireland: the PRIME study. Br J Nutr 2004;92:963–72.
[3] Hertog MG, Feskens EJ, Hollman PC, Katan MB, Kromhout D. Dietary antioxidant flavonoids and risk of coronary heart disease: the Zutphen Elderly Study. Lancet 1993;342:1007–11.
[4] Mink PJ, Scrafford CG, Barraj LM, Harnack L, Hong CP, Nettleton JA, et al. Flavonoid intake and cardiovascular disease mortality: a prospective study in postmenopausal women. Am J Clin Nutr 2007;85:895–909.
[5] Manach C, Scalbert A, Morand C, Remesy C, Jimenez L. Polyphenols: food sources and bioavailability. Am J Clin Nutr 2004;79:727–47.
[6] Ovaskainen ML, Torronen R, Koponen JM, Sinkko H, Hellstrom J, Reinivuo H, et al. Dietary intake and major food sources of polyphenols in Finnish adults. J Nutr 2008;138:562–6.
[7] Lee CH, Jeong TS, Choi YK, Hyun BH, Oh GT, Kim EH, et al. Anti-atherogenic effect of citrus flavonoids, naringin and naringenin, associated with hepatic ACAT and aortic VCAM-1 and MCP-1 in high cholesterol-fed rabbits. Biochem Biophys Res Commun 2001;284:681–8.
[8] Choe SC, Kim HS, Jeong TS, Bok SH, Park YB. Naringin has an antiatherogenic effect with the inhibition of intercellular adhesion molecule-1 in hypercholesterolemic rabbits. J Cardiovasc Pharmacol 2001;38:947–55.
[9] Mulvihill EE, Assini JM, Sutherland BG, DiMattia AS, Khami M, Koppes JB, et al. Naringenin decreases progression of atherosclerosis by improving dyslipidemia in high-fat-fed low-density lipoprotein receptor-null mice. Arterioscler Thromb Vasc Biol 2010;30:742–8.
[10] Jung UJ, Lee MK, Park YB, Kang MA, Choi MS. Effect of citrus flavonoids on lipid metabolism and glucose-regulating enzyme mRNA levels in type-2 diabetic mice. Int J Biochem Cell Biol 2006;38:1134–45.
[11] Mulvihill EE, Allister EM, Sutherland BG, Telford DE, Sawyez CG, Edwards JY, et al. Naringenin prevents dyslipidemia, apolipoprotein B overproduction, and hyperinsulinemia in LDL receptor-null mice with diet-induced insulin resistance. Diabetes 2009;58:2198–210.
[12] Huong DT, Takahashi Y, Ide T. Activity and mRNA levels of enzymes involved in hepatic fatty acid oxidation in mice fed citrus flavonoids. Nutrition 2006;22:546–52.
[13] Wilcox LJ, Borradaile NM, de Dreu LE, Huff MW. Secretion of hepatocyte apoB is inhibited by the flavonoids, naringenin and hesperetin, via reduced activity and expression of ACAT2 and MTP. J Lipid Res 2001;42:725–34.
[14] Borradaile NM, de Dreu LE, Barrett PH, Behrsin CD, Huff MW. Hepatocyte apoB-containing lipoprotein secretion is decreased by the grapefruit flavonoid, naringenin, via inhibition of MTP-mediated microsomal triglyceride accumulation. Biochemistry 2003;42:1283–91.
[15] Allister EM, Mulvihill EE, Barrett PH, Edwards JY, Carter LP, Huff MW. Inhibition of apoB secretion from HepG2 cells by insulin is amplified by naringenin, independent of the insulin receptor. J Lipid Res 2008;49:2218–29.
[16] Borradaile NM, de Dreu LE, Huff MW. Inhibition of net HepG2 cell apolipoprotein B secretion by the citrus flavonoid naringenin involves activation of phosphatidylinositol 3-kinase, independent of insulin receptor substrate-1 phosphorylation. Diabetes 2003;52:2554–61.
[17] Vafeiadou K, Vauzour D, Lee HY, Rodriguez-Mateos A, Williams RJ, Spencer JP. The citrus flavanone naringenin inhibits inflammatory signalling in glial cells and protects against neuroinflammatory injury. Arch Biochem Biophys 2009;484:100–9.
[18] Garcia-Conesa MT, Tribolo S, Guyot S, Tomas-Barberan FA, Kroon PA. Oligomeric procyanidins inhibit cell migration and modulate the expression of migration and proliferation associated genes in human umbilical vascular endothelial cells. Mol Nutr Food Res 2009;53:266–76.
[19] Stangl V, Dreger H, Stangl K, Lorenz M. Molecular targets of tea polyphenols in the cardiovascular system. Cardiovasc Res 2007;73:348–58.
[20] Paigen B, Morrow A, Brandon C, Mitchell D, Holmes P. Variation in susceptibility to atherosclerosis among inbred strains of mice. Atherosclerosis 1985;57:65–73.
[21] Li Y, Gilbert TR, Matsumoto AH, Shi W. Effect of aging on fatty streak formation in a diet-induced mouse model of atherosclerosis. J Vasc Res 2008;45:205–10.
[22] Paigen B, Morrow A, Holmes PA, Mitchell D, Williams RA. Quantitative assessment of atherosclerotic lesions in mice. Atherosclerosis 1987;68:231–40.
[23] Auclair S, Milenkovic D, Besson C, Chauvet S, Gueux E, Morand C, et al. Catechin reduces atherosclerotic lesion development in apo E-deficient mice: a transcriptomic study. Atherosclerosis 2009;204:e21–7.
[24] le Morvan V, Dumon MF, Palos-Pinto A, Berard AM. n-3 FA increase liver uptake of HDL-cholesterol in mice. Lipids 2002;37:767–72.
[25] Benzie IF, Strain JJ. The ferric reducing ability of plasma (FRAP) as a measure of "antioxidant power": the FRAP assay. Anal Biochem 1996;239:70–6.
[26] Nicoletti A, Kaveri S, Caligiuri G, Bariety J, Hansson GK. Immunoglobulin treatment reduces atherosclerosis in apoE knockout mice. J Clin Invest 1998;102:910–8.
[27] Berard AM, Foger B, Remaley A, Shamburek R, Vaisman BL, Talley G, et al. High plasma HDL concentrations associated with enhanced atherosclerosis in transgenic mice overexpressing lecithin-cholesteryl acyltransferase. Nat Med 1997;3:744–9.
[28] Beissbarth T, Speed TP. GOstat: find statistically overrepresented Gene Ontologies within a group of genes. Bioinformatics 2004;20:1464–5.
[29] Maier JA, Malpuech-Brugere C, Zimowska W, Rayssiguier Y, Mazur A. Low magnesium promotes endothelial cell dysfunction: implications for atherosclerosis, inflammation and thrombosis. Biochim Biophys Acta 2004;1689:13–21.
[30] Potier M, Karl M, Elliot SJ, Striker GE, Striker LJ. Response to sex hormones differs in atherosclerosis-susceptible and -resistant mice. Am J Physiol Endocrinol Metab 2003;285:E1237–45.

[31] Paigen B, Holmes PA, Mitchell D, Albee D. Comparison of atherosclerotic lesions and HDL-lipid levels in male, female, and testosterone-treated female mice from strains C57BL/6, BALB/c, and C3H. Atherosclerosis 1987;64:215–21.
[32] Brett GM, Hollands W, Needs PW, Teucher B, Dainty JR, Davis BD, et al. Absorption, metabolism and excretion of flavanones from single portions of orange fruit and juice and effects of anthropometric variables and contraceptive pill use on flavanone excretion. Br J Nutr 2009;101:664–75.
[33] Bredsdorff L, Nielsen IL, Rasmussen SE, Cornett C, Barron D, Bouisset F, et al. Absorption, conjugation and excretion of the flavanones, naringenin and hesperetin from alpha-rhamnosidase-treated orange juice in human subjects. Br J Nutr 2010;103:1602–9.
[34] Ishibashi S, Herz J, Maeda N, Goldstein JL, Brown MS. The 2-receptor model of lipoprotein clearance — tests of the hypothesis in knockout mice lacking the low-density-lipoprotein receptor, apolipoprotein-E, or both proteins. Proc Natl Acad Sci U S A 1994;91:4431–5.
[35] Mahley RW, Ji ZS, Brecht WJ, Miranda RD, He D. Role of heparan sulfate proteoglycans and the LDL receptor-related protein in remnant lipoprotein metabolism. Ann N Y Acad Sci 1994;737:39–52.
[36] Spertini O, Luscinskas FW, Kansas GS, Munro JM, Griffin JD, Gimbrone Jr MA, et al. Leukocyte adhesion molecule-1 (LAM-1, L-selectin) interacts with an inducible endothelial cell ligand to support leukocyte adhesion. J Immunol 1991;147: 2565–73.
[37] Pendu R, Terraube V, Christophe OD, Gahmberg CG, de Groot PG, Lenting PJ, et al. P-selectin glycoprotein ligand 1 and beta2-integrins cooperate in the adhesion of leukocytes to von Willebrand factor. Blood 2006;108:3746–52.
[38] Barlic J, Murphy PM. Chemokine regulation of atherosclerosis. J Leukoc Biol 2007;82:226–36.
[39] Hordijk PL. Endothelial signalling events during leukocyte transmigration. FEBS J 2006;273:4408–15.
[40] Carman CV, Springer TA. A transmigratory cup in leukocyte diapedesis both through individual vascular endothelial cells and between them. J Cell Biol 2004;167:377–88.
[41] Cho T, Jung Y, Koschinsky ML. Apolipoprotein(a), through its strong lysine-binding site in KIV(19′), mediates increased endothelial cell contraction and permeability via a Rho/Rho kinase/MYPT1-dependent pathway. J Biol Chem 2008;283:30503–12.
[42] Jacobson JR, Dudek SM, Birukov KG, Ye SQ, Grigoryev DN, Girgis RE, et al. Cytoskeletal activation and altered gene expression in endothelial barrier regulation by simvastatin. Am J Respir Cell Mol Biol 2004;30:662–70.
[43] Koss M, Pfeiffer II GR, Wang Y, Thomas ST, Yerukhimovich M, Gaarde WA, et al. Ezrin/radixin/moesin proteins are phosphorylated by TNF-alpha and modulate permeability increases in human pulmonary microvascular endothelial cells. J Immunol 2006;176:1218–27.
[44] Schnoor M, Parkos CA. Disassembly of endothelial and epithelial junctions during leukocyte transmigration. Front Biosci 2008;13:6638–52.
[45] Broman MT, Kouklis P, Gao X, Ramchandran R, Neamu RF, Minshall RD, et al. Cdc42 regulates adherens junction stability and endothelial permeability by inducing alpha-catenin interaction with the vascular endothelial cadherin complex. Circ Res 2006;98:73–80.
[46] Heasman SJ, Ridley AJ. Mammalian Rho GTPases: new insights into their functions from *in vivo* studies. Nat Rev Mol Cell Biol 2008;9:690–701.
[47] Kundumani-Sridharan V, Wang D, Karpurapu M, Liu Z, Zhang C, Dronadula N, et al. Suppression of activation of signal transducer and activator of transcription-5B signaling in the vessel wall reduces balloon injury-induced neointima formation. Am J Pathol 2007;171:1381–94.
[48] Yoon JJ, Lee YJ, Kim JS, Kang DG, Lee HS. Betulinic acid inhibits high glucose-induced vascular smooth muscle cells proliferation and migration. J Cell Biochem 2010;111:1501–11.
[49] Chen S, Gardner DG. Suppression of WEE1 and stimulation of CDC25A correlates with endothelin-dependent proliferation of rat aortic smooth muscle cells. J Biol Chem 2004;279:13755–63.
[50] Onda M, Naito Z, Wang R, Fujii T, Kawahara K, Ishiwata T, et al. Expression of keratinocyte growth factor receptor (KGFR/FGFR2 IIIb) in vascular smooth muscle cells. Pathol Int 2003;53:127–32.